SWITCHABLE MICROWAVE BAND-STOP TO ALL PASS FILTER USING STEPPED IMPEDANCE RESONATOR

Amine A. Bakhit[*] and Peng W. Wong

Department of Electrical and Electronics Engineering, Universiti Teknologi PETRONAS, Bandar Seri Iskandar, Tronoh, Perak 31750, Malaysia

Abstract—Electronically switchable microwave filters are attracting more attention for research and development because of their importance in increasing the capability of wireless communication and cognitive radios. In this paper, novel switchable microwave band-stop to all pass filters are designed by using stepped impedance resonator. Commercially available Pin diodes are used in order to allow the fastest switching between band-stop and all pass responses. The theoretical analysis is presented in this paper, and its feasibility has been experimentally verified with a micro-strip prototype. The design was also characterized by measuring the filter performance with increasing power levels of 20, 15, 10, 5, and 0 dBm. The results have shown that the switchable filter is immune to power saturation effects. Nonlinear measurements at higher power levels are also performed and the switchable filter produced low power inter-modulation product. The main advantage of this filter is its capability to switch between band-stop and all pass mode of operation. Other advantages include being small in size, and low in cost.

1. INTRODUCTION

As modern wireless and microwave systems progress towards a spectral cognitive system, increasingly high filter re-configurability will be necessary in order to fully utilize the potential of the system's performance [1]. The first condition that must be met by a reconfigurable filter is that it must be capable of inducing microwave transmitters and receivers that are adaptable to multi-band operations using a single filter, which is highly desirable in the current wireless

communication technology. Among the many techniques found in recent literature, switchable filters for cognitive system prove to be a popular technique, because of their flexibility and ability to display more than one response in a controllable manner. In addition, cognitive radio is able to sense the available spectrum and configure the communication channel to use [21, 22]. Unlike conventional wireless communication systems, this radio does not need to have an allocated fixed frequency bands and the use of switched filter bank that covers the whole spectrum tremendously increase the system complexity, size and cost. Therefore, reconfigurable or switchable microwave filters can be the key components in increasing the capability of wireless communication and cognitive radios architectures and will also greatly simplify the front end architecture.

Hunter et al. [2] suggested that quite a number of microwave front ends are primarily designed with band pass filters in order to prevent it from generating or receiving unwanted interference. The omnipresence of band pass filters is due to the fact that most microwave systems are rendered unaware of the spectrum they are operating in, which creates a need for a fear-based front-end architecture attenuating all frequencies except the band of interests. However, a front-end architecture based on band pass filters results in a significant insertion loss in the frequency band of interest, which scuttle the system's performance. There is an embedded trade-off between the given resonator quality factor (Q), band pass filter bandwidth, order, and the pass band insertion loss [3]. Therefore, the greater the protection from generating or receiving interference in the adjacent frequency bands, the higher the insertion loss will be in the band of interest. When compared to band pass filters, the band-stop filters exhibit lower pass band insertion losses, which minimizes the degradation of the receiver's noise figure, while providing a high rejection level in removing spurious signals. Therefore, recent interest in tunable band-stop filter for cognitive system is skyrocketing [4–9]. These band-stop filters are salient in spectral-dense environment, where high power interference signal is of a primary concern. Also, band-stop filters are used for spectral management by compressing jammer level in the receiver radio and are essential in the software defined radio and cognitive radio systems.

As depicted in Figure 1, it is assumed that there is a specific bandwidth BW GHz in the frequency range of [0–3.75] GHz and it is available for use in a wide-band wireless network. Being cognitive, this network supports different wireless technology over different frequency bands. Moreover, if it is assumed that there are multiple cognitive radios, simultaneously operating in the assumed frequency range,

increasingly a dynamic filter shape may be needed by a new radio for it to effectively join the environment. If this frequency range does contain several higher power interfering signals that are, spectrally close to the receive bands as depicted in Figure 1; the radio may lose its ability to resolve desired signals well. In this situation, the SNR could possibly be maximized if the radio was able to place a deep band-stop filter response at the higher power interference frequency of operation.
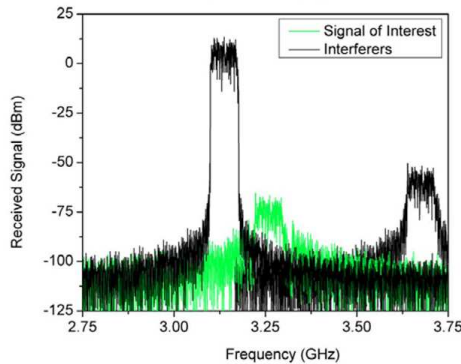

Figure 1. Spectrum where a band-rejct filter would be most useful for attenuating the interfering signals. These signals were adapted from an Agilent ADS example WCDMA project [5].

Microwave system that is cognizant of the spectrum in which it is operating [1], would not need to operate in the fear-based mode of operation described above. In fact, it could operate without a filter if there was no strong interference. This would greatly benefit lower insertion loss than band-pass-centric front ends [23].

Wide-band systems [10], and systems with highly linear low-noise amplifiers (LNAs) [11] could reap the most benefit from such an interference mitigation strategy; which allows a receiver to take advantage of the benefits of a band-stop filter-centric front end, while dynamically allowing for a mode of operation that allows signals at all frequencies to be received when there are no interferences. Such an electronically switchable microwave filter is also desirable for multi-band telecommunication system, radio-meters, wide-band radar or electronically welfare communication systems, because of their diversity and high integration.

From the discussion above, it can be seen that filters are very important components for modern microwave transmitters and receivers. They occupy relatively large amount of physical space in modern wireless systems when compared to other typical radio

components, most of which are now easily integrated on chip. Usually, they are placed before amplifiers, balanced mixers and antenna feeds. Nowadays, applications such as cognitive radio and wireless system usually require small device in order to meet the miniaturization requirement of current devices. However, in many cases, it would be impractical to implement both tunable band-stop filter banks and tunable all pass filter banks in a filter due to system size constraints. A possible solution to this problem is to implement sets of coupled resonators, in which response can be dynamically switched between a band-stop and all pass filter shape. This is not only saves space but adds flexibility to a system.

Figure 2 shows that Chebyshev band-pass, elliptic band-pass and band-stop responses can be obtained from the same set of resonator if their coupling values are tunable. The dashed lines represent tunable or switchable coupling values while the solid line represents static coupling. It was noted that Figure 2 is theoretical and the ability to achieve all these responses would require components that have a wider tuning ranges than those commercially available today.
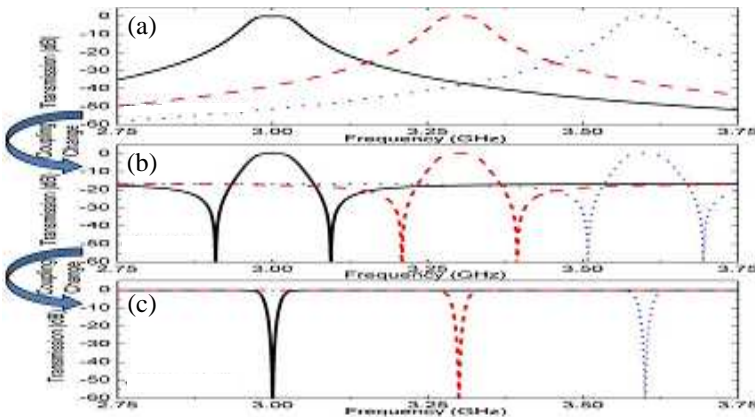

Figure 2. Simulated results show possible responses of a set of two tunable resonators with tunable external and/or source-load coupling values [5]. (a) Chebyshev, (b) elliptic, (c) band-stop.

Naglish et al. [5] presented a new band pass to band-stop tunable filter. Tu [12] created a filter with the ability to switch between Chebyshev band-pass, elliptic band-pass, and off response. In contrast as presented in this work, the filter switches between the designed band-pass and band-stop filter responses, which is a fundamentally different functionality.

In 2006, Karim et al. [13] and in 2009, Chen et al. [14] achieved a band-pass to band-stop electronically reconfigurable filter. However, the filters demonstrated theirs work are not tunable and use relatively low Q resonators that result in spectrally wide responses. The filter by Karim et al. [13] uses the frequency selective behavior of a cascade of unit electromagnetic band gap (EBG) structures that can be switched [14], and demonstrates a band-pass to band-stop filter with a closed ring resonators, which can be re-configured by the perturbation effect on degenerate modes.

Until recently, different structures of micro-strip reconfigurable or switchable filters have been developed [12–14, 23–29]. These structures are all innovative; but a switchable microwave band-stop to all pass filters using stepped impedance resonator and suitable to be integrated into a switchable, narrow band system has not yet been demonstrated. This paper is concerned with the design of a novel switchable microwave filter using stepped impedance resonator with new capabilities unfounded in previous designs.

This paper is organized as follows; Section 2 discusses the band-stop to all pass filter design, while the micro-strip prototype and measurements is presented in Section 3. The filter performance with increasing power level is presented in Section 4 and followed by low power intermodulation performance measurements in Section 5. Finally, the work is summarized in Section 6.

2. BAND-STOP TO ALL PASS FILTER DESIGN

This section is divided into two parts in order to investigate the switchability of band-stop to all pass filter. Section 2.1 introduces the theoretical analysis of the design by using stepped impedance resonator. Section 2.2 presents the Matlab simulation results of the proposed design by using the classical even and odd mode analysis.

2.1. Theoretical Analysis of the Design

In a cognitive radio spectrum utilization scheme, it is useful to switch off the band-stop filter in case no interference is present. When the filter is switched off, additional channel loss introduced by the filter will be minimized and the available wireless spectrum will be fully utilized [17].

In this work, PIN diode switches are incorporated into the miniaturized matched band-stop filter topology [16] in order to realize the design of a band-stop to all pass filters. Therefore, the novel capacitive coupling structure type of filter is shown in the circuit of

Figure 3. It can be seen in Figure 3(a) that the low z sections of both the left and right sides have an electrical length of (θ_x) and a characteristic impedance of Z_2. The high Z sections of both the left and right sides have an electrical length of (θ_y) and characteristic impedance of Z_1. Moreover, the resonator is loaded with a lump-coupling element L, where the lump inductor is shunted at the midpoint of the transmission line section. Finally, the input and output is coupled by an inverter $K_3 = 90°$.
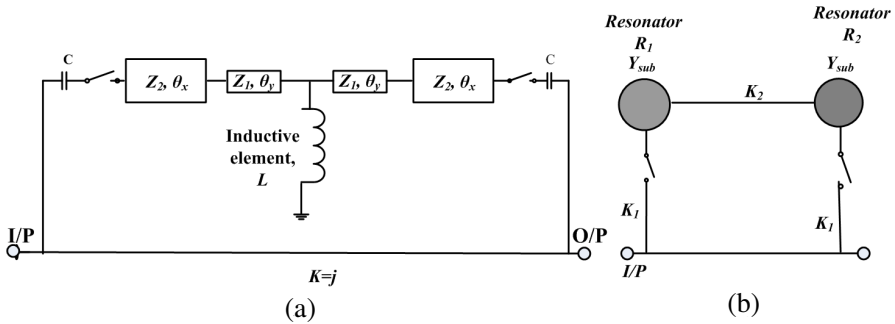

Figure 3. (a) Coupling structure in the band-stop to all pass mode filter, (b) generalized coupled resonator model for band-stop to all pass filter.

This coupling structure provides two modes of operation under two conditions. In the first condition, the PIN diodes are switched "ON". During the "ON" state, the PIN diode behaves like a variable resistor, R_s, for high-frequency signal. Therefore, the new capacitive coupling structure for this mode of operation, along with its generalized coupled resonator model, is displayed in Figures 4(a) and 4(b). This topology is a symmetrical structure with respect to the plane AA', which ensures that the resonance condition can be derived by utilizing the classical method for odd and even mode analysis. The even and odd mode admittances of the generalized coupled resonator model shown in Figure 4(b) are derived as follows:

$$Y_{even}(p) = -j + R_s K_1^2 + \frac{K_1^2}{Y_{sub} + jK_2} \tag{1}$$

and

$$Y_{odd}(p) = +j + R_s K_1^2 + \frac{K_1^2}{Y_{sub} - jK_2} \tag{2}$$

where Y_{sub} is the characteristic impedance of the resonator, K_1 the coupling between the input and the resonator, and K_2 the coupling between the resonator.
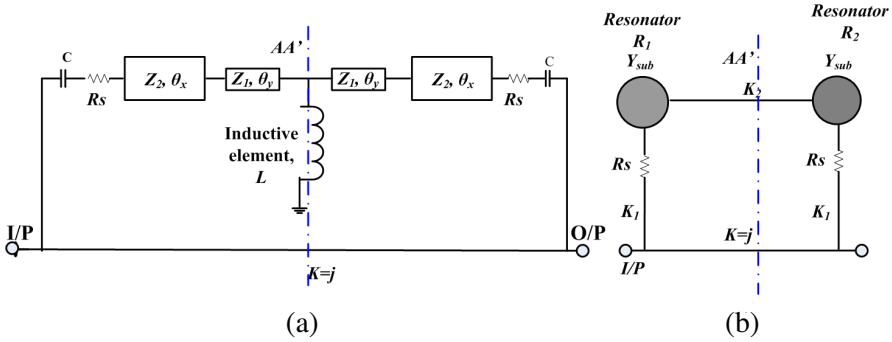
Figure 4. (a) Coupling structure of the miniaturized matched band-stop mode of operation, (b) generalized coupled resonator model for band-stop mode of operation.

The transmission and reflection function of the filter can be calculated from the odd and even mode admittances [15, 30] and are given as:

$$S(1,2) = \frac{Y_{odd}(p) - Y_{even}(p)}{(1 + Y_{odd}(p))(1 + Y_{even}(p))} \tag{3}$$

$$S(1,1) = \frac{1 - Y_{odd}(p)Y_{even}(p)}{(1 + Y_{odd}(p))(1 + Y_{even}(p))} \tag{4}$$

For a perfectly matched system at resonance

$$S(1,2)|_{\omega_0} = 0 \Rightarrow Y_{odd}(p) - Y_{even}(p) = 0 \tag{5}$$

and

$$S(1,1)|_{\omega_0} = 0 \Rightarrow Y_{odd}(p) = \frac{1}{Y_{even}(p)} \tag{6}$$

The values of K_1 and K_2 are derived from Equations (5) and (6) as follows:

$$K_1 = \pm \frac{-1 + \sqrt{-K_2 \left(2 + 4R_sG + 2R_s^2G^2 + 2R_s^2K_2^2\right)}}{2\left(1 + 2R_sG + R_s^2G^2 + R_s^2K_2^2\right)} \tag{7}$$

$$K_2 = \pm \frac{-1 + \sqrt{1 - 4R_s^2G^2 - R_sG}}{2(R_s)} \tag{8}$$

When the forward resistance R_s, is equal to zero; the generalized coupling resonator models shown in Figure 5(b) will have similar structure as the Generalized coupled resonator model of a matched notch filter, displayed in [18, 19], and the expression of K_1 and K_2 in
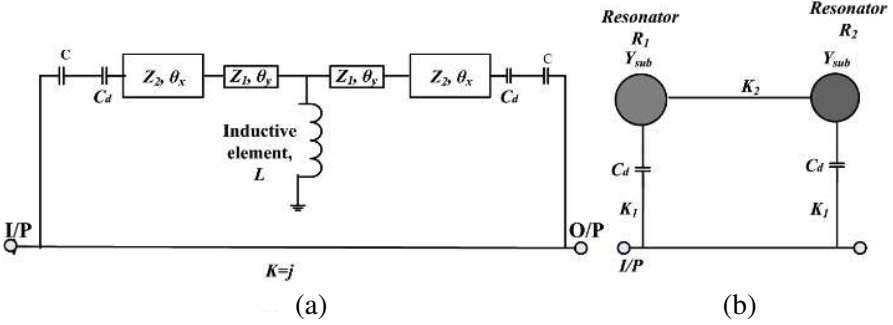
Figure 5. (a) Coupling structure for an all pass mode of operation, (b) generalized coupled resonator model for an all pass mode of operation.

Equations (7) and (8) can be obtained when the forward resistance of the pin diode R_s tend to zero as follows:

$$\lim_{Rs \to 0} (K_2) = \pm G.$$

and

$$\lim_{Rs \to 0} (K_1) = \pm \sqrt{2G}.$$

In the second condition, the PIN diodes are switched "OFF". With "OFF" state, the PIN diode acts as a low capacitance C_d. The capacitive coupling structure of this mode of operation and its generalized coupled resonator model are displayed in Figure 5. This mode of operation provides an all passes responses.

2.2. Simulation Results

The proposed prototype was analytically investigated using Mat-lab simulation. The Scattering coefficients of the band-stop mode of the filter are shown in Figure 6 with the forward resistance R_s equal to 0, and 0.02 ohm. The return loss $S(1,1)$ is infinite when the forward resistance R_s is equal to 0. Furthermore, the insertion loss $S(1,2)$ is infinite at resonance frequency of the filter.

When R_s is finite, it can be seen that the return loss $S(1,1)$ is around 80 dB within the pass band of interest, and infinite at resonance frequency of the filter. Furthermore, the insertion $S(1,2)$ is infinite at the resonance frequency of this filter.
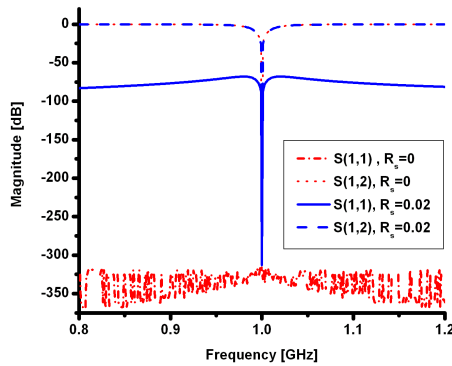
Figure 6. Simulated band-stop mode responses of the proposed prototype when the forward resistance $R_s = 0$, and 0.02 ohm.

3. MICRO-STRIP PROTOTYPE

Switchable band-stop to all pass filter based on the stepped impedance dual mode resonator was designed and fabricated on a Rogers RT/Duroid 5880 substrate, with a dielectric constant of 2.2 and a thickness of 787 µm. Simulations were carried out by an EM-simulator ADS. The scattering parameters are measured by Agilent network analyzers. The micro-strip circuit prototype is shown in Figure 7(a).

To employ a pin diode as RF switch, a biasing network similar to the one shown in Figure 7(b) [20] is necessary, where C is the DC
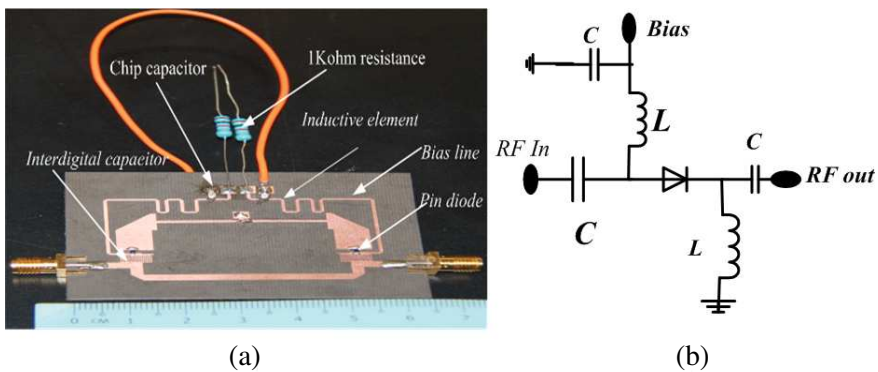

(a)   (b)

Figure 7. (a) Photography of switchable band-stop to all pass filters, (b) pin diode biasing network [20].

blocking capacitor and L is the RF choke. This ensures minimum isolation between the DC biasing circuit and the miniaturized RF circuitry at the operating frequency. The value of C is chosen to provide lowest reactance (possible highest capacitance) while still ensuring that the self resonance of the opponent is greater than the operating frequency of the filter. This provides lowest resistance for RF signal while blocking the DC biasing. The value of L is chosen to provide highest reactance (possibly highest inductance) while still ensuring that the self resonance of the opponent is greater than the operating frequency of the filter. This provides lowest resistance for DC signal while blocking the RF signal.

The switch elements used in this design are sky-work SMP1345 in an SC79 package. They have a frequency range of 10 MHz to 6 GHz, a low-forward resistance (1.5 ohm at 10 mA), and very low capacitance (0.15 pF) in reverse bias mode. The inductive element is realized by a short circuit via a hole shunted at the mid-point of the resonator. The high-impedance quarter-wave-length transmission-line elements of 200 μm wide (100 ohm) micro-strip traces were implemented in order to provide bias to the Pin diodes, in conjunction with 1 Kohm resistance, and 100 pF chip capacitors. The coupling between the input/output and the resonator of the proposed prototype was obtained by an inter-digital capacitor available in Agilent Advanced Design System (ADS).

3.1. Pin Diodes Are Switched "*ON*"

The operation of the filter is based on the PIN diodes "ON" and "OFF" mode. When the pin diodes are switched "ON", the filter produces a matched band-stop response. The pin diode switches are turned "ON" when 10 V is connected to the bias line. The measured frequency
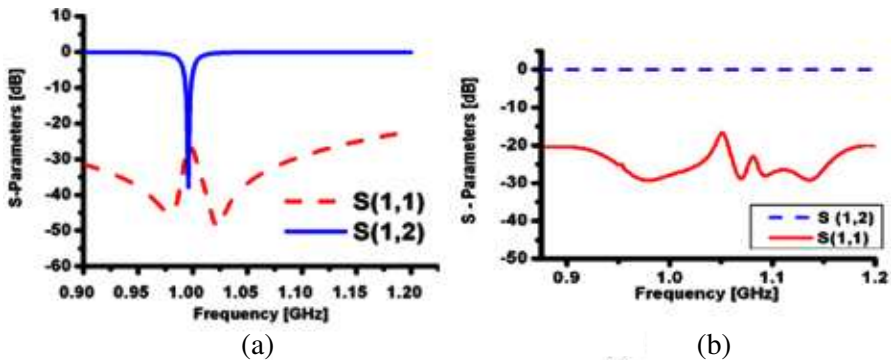

Figure 8. (a) Measured band-stop mode of operation, (b) measured all pass mode of operation.

responses of insertion loss $S(2,1)$, and return loss $S(1,1)$ are shown in Figure 8(a). The insertion loss is around 38 dB and the return loss is around 27 dB.

3.2. Pin Diodes Are Switched "*OFF*"

When the pin diodes are turned "OFF", the filter produces an All-Pass response. The measured frequency responses of $S(2,1)$ and $S(1,1)$ magnitudes are shown in Figure 8(b). It can be seen that the transmission response is totally flat at 0 dB, and the reflection coefficient response is around −17 dB.

4. LARGE SIGNALS CHARACTERIZATION

The fabricated switchable microwave filter was characterized by measuring the filter performance with increasing power levels. The measurements were performed using Vector Network Analyzers from Agilent Technologies, available at the department of Electrical and Electronics Engineering of Universiti Teknologi PETRONAS. It can be seen in Figure 9 that the proposed filter is immune from power saturation effect.
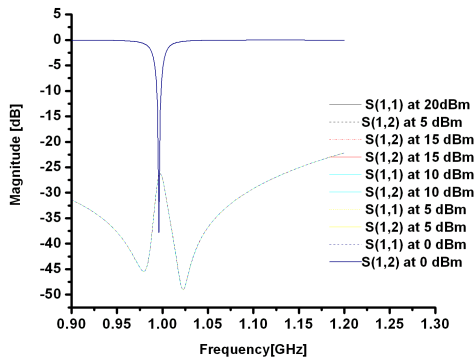

Figure 9. The filter performance with increasing power level of 20, 15, 10, 5, and 0 dBm.

5. LOW POWER INTERMODULATION PERFORMANCE MEASUREMENT

Due to non linearity of the pin diode switch it is important to measure the amount of signal distortion of switchable band-stop to all pass

filters using the measurement setup shown in Figure 10. The inter-modulation of the switchable filter was measured around the center frequency of the filter f_0. First, two signals with frequencies $f_1 = f_0 - \delta f/2$ and $f_2 = f_0 + \delta f/2$ were considered with a signals combiner and kept at the same power levels. The signal frequency separation was varied by $\delta f = 100\,\text{kHz}$, $50\,\text{kHz}$, $25\,\text{kHz}$. These two signals were then delivered to the device under the test (DUT) with input power levels of 15, 10, 5, and $0\,\text{dBm}$. In this measurement setup, the inter-modulation products are observed at the output spectrum of the switchable filter and can be found at the frequencies $2f_1 - f_2$ and $2f_2 - f_1$.
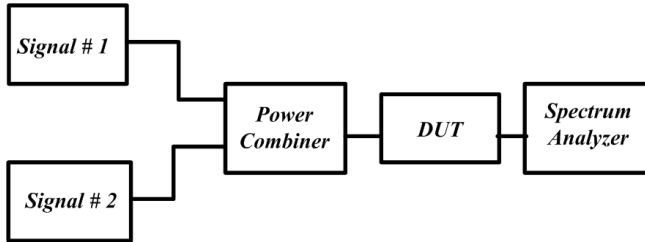

Figure 10. Setup configuration for the measurement of the low power intermodulation performance.

Figure 11 shows the output spectrum with two signals test with frequency separation $\delta f = 100\,\text{kHz}$, and input power level of 0, 5, 10, and $15\,\text{dBm}$. Similar experiment is conducted using the measurement setup depicted in Figure 10 with frequency separation $\delta f = 50\,\text{kHz}$, $25\,\text{kHz}$. The output results of this experiments are recorded and summarized in Table 1, Table 2, and Table 3 in which P (dBm) is the output power of the fundamental signal and IMD is the output power of the third order intermodulation products.

It can be seen in Figure 11 that the switchable band-stop filter produced low intermodulation product. Filters using RF

Table 1. Two signals and inter-modulation components level with frequency separation of $100\,\text{kHz}$ and input power of 15, 10, 5, and $0\,\text{dBm}$.

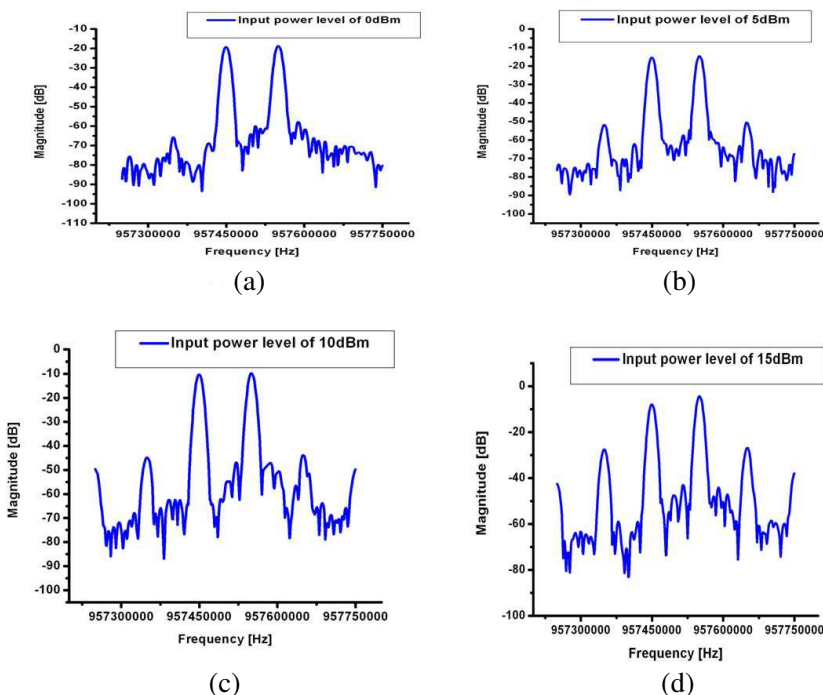| Input Power	IMD#1	P#1	P#2	IMD#2
$0\,\text{dBm}$	$-69.95\,\text{dBm}$	$-19.2\,\text{dBm}$	$-18.95\,\text{dBm}$	$-69.85\,\text{dBm}$
$5\,\text{dBm}$	$-54.75\,\text{dBm}$	$-14.25\,\text{dBm}$	$-14.05\,\text{dBm}$	$-50.5\,\text{dBm}$
$10\,\text{dBm}$	$-40.5\,\text{dBm}$	$-9.2\,\text{dBm}$	$-8.97\,\text{dBm}$	$-40.15\,\text{dBm}$
$15\,\text{dBm}$	$-25.3\,\text{dBm}$	$-4.35\,\text{dBm}$	$-4.3\,\text{dBm}$	$-25.04\,\text{dBm}$

Figure 11. Measured output spectrum with two tones test with frequency separation $\delta f = 100\,\text{kHz}$ and input power of 15, 10, 5, 0 dBm.

Table 2. Two signals and inter-modulation components level with frequency separation of 50 kHz and input power of 15, 10, 5, and 0 dBm.

Input Power	IMD#1	P#1	P#2	IMD#2
0 dBm	$-69.45\,\text{dBm}$	$-19.89\,\text{dBm}$	$-20.89\,\text{dBm}$	$-69.88\,\text{dBm}$
5 dBm	$-54.39\,\text{dBm}$	$-14.85\,\text{dBm}$	$-14.85\,\text{dBm}$	$-54.65\,\text{dBm}$
10 dBm	$-40.45\,\text{dBm}$	$-9.63\,\text{dBm}$	$-9.66\,\text{dBm}$	$-43.15\,\text{dBm}$
15 dBm	$-24.55\,\text{dBm}$	$-4.81\,\text{dBm}$	$-4.84\,\text{dBm}$	$-24.65\,\text{dBm}$

MEMS switches typically have better linearity in which case the intermodulation product is expected to be lower. However, the filter presented here results in no significant signal distortion and is immune from power saturation effects.

Table 3. Two signals and inter-modulation components level with frequency separation of 25 kHz and input power of 15, 10, 5, and 0 dBm.

Input Power	IMD#1	P#1	P#2	IMD#2
0 dBm	-66.45 dBm	-23.4 dBm	-23.06 dBm	-66.88 dBm
5 dBm	-51.29 dBm	-22.75 dBm	-22.8 dBm	-51.65 dBm
10 dBm	-35.45 dBm	-22.63 dBm	-22.65 dBm	-35.15 dBm
15 dBm	-20.55 dBm	-22.81 dBm	-22.74 dBm	-20.75 dBm

6. CONCLUSION

Switchable microwave filter has been designed, fabricated and tested. This filter is realized by using stepped impedance resonator, with Pin diodes incorporated into the topology as switching elements. It provides two modes of operation under two conditions; in the first condition, the filter produced a band-stop response when the pin diodes were switched "ON", and the filter produced an all pass response when the Pin diodes were switched "OFF". Theoretical analysis of the approach is presented, and the feasibility of the approach has been experimentally verified with a micro-strip circuit prototype.

The results clearly indicate that the filtering capability and flexibility provided by band-stop-to-all-pass filters enables new high-frequency front end strategies featuring very low pass band insertion loss. In addition, the fabricated filter was characterized by measuring the filter performance with increasing power level. Furthermore, the results have shown that the filter is immune from power saturation effect. Nonlinear measurements at higher power levels are also performed and the switchable filter produced a low power inter-modulation.

The benefits and applications of a switchable band-stop to an all-pass filter are envisioned to include general system flexibility, at no cost of physical space. In wireless communication and cognitive radio environments, these filters would be invaluable to radio systems. It allows the receiver to take advantage of the benefits of a band-stop filter centric front end, while dynamically allowing for a mode of operation, which allows signal at all frequencies to be received when there are no interference. Such an electronically switchable band-stop to all pass filter is also desirable for wide-band radar or electronically welfare system.

REFERENCES

1. Perlman, B., J. Laskar, and K. Lim, "Fine-tuning commercial and military radio design," *IEEE Microw. Mag.*, Vol. 9, No. 4, 95–106, Aug. 2008.

2. Hunter, I., R. Ranson, A. Guyette, and A. Abunjaileh, "Microwave filter design from a systems perspective," *IEEE Microw. Mag.*, Vol. 8, No. 5, 71–77, Oct. 2007.

3. Hunter, I. C., *Theory and Design of Microwave Filters*, Ch. 4, 125–131, Inst. Electr. Eng., London, UK, 2001.

4. Jachowski, D. R. and C. Rauscher, "Frequency-agile bandstop filter with tunable attenuation," *IEEE MTT-S Int. Microw. Symp. Dig.*, 649–652, Boston, MA, Jun. 2009.

5. Naglich, E. J., J. Lee, D. Peroulis, and W. J. Chappell, "A tunable bandpass-to-bandstop reconfigurable filter with independent bandwidths and tunable response shape," *IEEE Trans. on Microw. Theory and Tech.*, Vol. 58, No. 12, 3770–3779, Dec. 2010.

6. Reines, I., S.-J. Park, and G. Rebeiz, "Compact low-loss tunable-band bandstop filter with miniature RF-MEMS switches," *IEEE Trans. on Microw. Theory and Tech.*, Vol. 58, No. 7, 1887–1895, Jul. 2010.

7. Yan, W. and R. Mansour, "Compact tunable bandstop filter integrated with large deflected actuators," *IEEE MTT-S Int. Microw. Symp. Dig.*, 1611–1614, Jun. 2007.

8. Tsai, C., G. Qiu, H. Gao, L. Yang, G. Li, S. Nikitov, and Y. Gulyaev, "Tunable wideband microwave band-stop and bandpass filters using YIG/GGG-GaAs layer structures," *IEEE Trans. on Magn.*, Vol. 41, No. 10, 3568–3570, Oct. 2005.

9. Rauscher, C., "Varactor-tuned active notch filter with low passband noise and signal distortion," *IEEE Trans. on Microw. Theory and Tech.*, Vol. 49, No. 8, 1431–1437, Aug. 2001.

10. Rodenbeck, C., S.-G. Kim, W.-H. Tu, M. Coutant, S. Hong, M. Li, and K. Chang, "Ultra-wideband low-cost phased-array radars," *IEEE Trans. on Microw. Theory and Tech.*, Vol. 53, No. 12, 3697–3703, Dec. 2005.

11. Kobayashi, K., Y. C. Chen, I. Smorchkova, R. Tsai, M. Wojtowicz, and A. Oki, "A 2 watt, sub-dB noise figure GaN MMIC LNA-PA amplifier with multi-octave bandwidth from 0.2–8 GHz," *IEEE MTT-S Int. Microw. Symp. Dig.*, 619–622, Jun. 2007.

12. Tu, W.-H., "Switchable microstrip bandpass filters with reconfigurable on-state frequency responses," *IEEE Microw.*

Wireless Compon. Lett., Vol. 20, No. 5, 259–261, May 2010.

13. Karim, M. F., A. Q. Liu, A. Alphones, and A. B. Yu, "A novel reconfigurable filter using periodic structures," *IEEE MTT-S Int. Microw. Symp. Dig.*, 943–946, San Francisco, CA, Jun. 2006.

14. Chen, Y.-M., S.-F. Chang, C.-Y. Chou, and K.-H. Liu, "A reconfigurable bandpass-bandstop filter based on varactor-loaded closed-ring resonators," *IEEE Microw. Mag.*, Vol. 10, No. 1, 138–140, Feb. 2009.

15. Hunter, I. C., *Theory and Design of Microwave Filters*, IEE, London, UK, 2001.

16. Bakhit, A. A. and P. W. Wong, "Miniaturized matched band-stop filter based dual-mode resonator," *National Postgraduate Conference (NPC)*, 1–3, Perak, Malaysia, Sep. 2011.

17. Wu, Z. Z., Y. Shim, and M. Rais-Zadeh, "Switchable wide tuning range bandstop filters for frequency-agile radios," *2011 IEEE International Electron Devices Meeting (IEDM)*, 2051–2054, Dec. 2011.

18. Bakhit, A. A. and P. W. Wong, "A novel single and dual-band miniaturized matched band-stop filter using stepped impedance resonator," *Progress In Electromagnetics Research C*, Vol. 33, 229–241, 2012.

19. Wong, P. W., I. C. Hunter, and R. D. Pollard, "Matched bandstop resonator with tunable K-inverter," *European Microwave Conference, 2007*, 664–667, Oct. 9–12, 2007.

20. Watertown, M., *The Pin Diode Circuit Designers' Handbook*, Microsemi Corporation, Sam, CA, Jul. 1992.

21. Mitola, J. and C. Q. Maguire, "Cognitive radio: Making software radio more personal," *IEEE Personal Communication Mag.*, Vol. 6, No. 4, 13–18, Aug. 1998.

22. Adoum, B. A. and V. Jeoti, "Cyclostationary feature based multiresolution spectrum sensing approach for DVB-T and wireless microphone signals," *2010 International Conference on Computer and Communication Engineering (ICCCE)*, 1–6, May 11–12, 2010.

23. Naglich, E. J., J. Lee, D. Peroulis, and W. J. Chappell, "Switchless tunable bandstop-to-all-pass reconfigurable filter," *IEEE Trans. on Microw. Theory and Tech.*, Vol. 60, No. 5, 1258–1265, May 2012.

24. Ourir, A., R. Abdeddaim, and J. de Rosny, "Tunable trapped mode in symmetric resonator designed for metamaterials," *Progress In Electromagnetics Research*, Vol. 101, 115–123, 2010.

25. Chao, S.-F., C.-H. Wu, Z.-M. Tsai, H. Wang, and C. H. Chen, "Electronically switchable bandpass filters using loaded stepped-impedance resonators," *IEEE Trans. on Microw. Theory and Tech.*, Vol. 54, 4193–4201, Dec. 2006.

26. Ning, H., J. Wang, Q. Xiong, and L.-F. Mao, "Design of planar dual and triple narrow-band bandstop filters with independently controlled stop bands and improved spurious response," *Progress In Electromagnetic Research*, Vol. 131, 259–274, 2012.

27. Wong, P. W. and I. C. Hunter, "Electronically tunable filters with constant absolute bandwidth," *IEEE Microw. Mag.*, Vol. 10, No. 6, 46–54, Oct. 2009.

28. Wong, P. W. and I. C. Hunter, "Electronically reconfigurable microwave bandpass filter," *IEEE Trans. on Microw. Theory and Tech.*, Vol. 57, No. 12, 3070–3079, Dec. 2009.

29. Wong, P. W. and I. C. Hunter, "A new class of low-loss high-linearity electronically reconfigurable microwave filter," *IEEE Trans. on Microw. Theory and Tech.*, Vol. 56, No. 8, 1945–1953, Aug. 2008.

30. Wong, P. W., "Miniaturized dual mode microwave filter," *2010 Asia-Pacific Microwave Conference Proceedings (APMC)*, 1090–1093, Dec. 7–10, 2010.